The Journal of Neuroscience, October 1, 1998, *18*(19):7662–7673

Morphologically Docked Synaptic Vesicles Are Reduced in *synaptotagmin* Mutants of *Drosophila*

Noreen E. Reist,[1] JoAnn Buchanan,[2] Jing Li,[2] Aaron DiAntonio,[2] Elizabeth M. Buxton,[1] and Thomas L. Schwarz[2]

[1]Department of Anatomy and Neurobiology, Colorado State University, Fort Collins, Colorado 80523, and [2]Department of Molecular and Cellular Physiology, Stanford University School of Medicine, Stanford, California 94305

Nerve terminal specializations include mechanisms for maintaining a subpopulation of vesicles in a docked, fusion-ready state. We have investigated the relationship between synaptotagmin and the number of morphologically docked vesicles by an electron microscopic analysis of *Drosophila synaptotagmin* (*syt*) mutants. The overall number of synaptic vesicles in a terminal was reduced, although each active zone continued to have a cluster of vesicles in its vicinity. In addition, there was an increase in the number of large vesicles near synapses. Examining the clusters, we found that the pool of synaptic vesicles immediately adjacent to the presynaptic membrane, the pool that includes the docked population, was reduced to 24 ± 5% (means ± SEM) of control in the syt^{null} mutation.

To separate contributions of overall vesicle depletion and increased spontaneous release from direct effects of synaptotagmin on morphological docking, we examined *syt* mutants in an altered genetic background. Recombining *syt* alleles onto a second chromosome bearing an as yet uncharacterized mutation resulted in the expected decrease in evoked release but suppressed the increase in spontaneous release frequency. Motor nerve terminals in this genotype contained more synaptic vesicles than control, yet the number of vesicles immediately adjacent to the presynaptic membrane near active zones was still reduced (33 ± 4% of control).

Our findings demonstrate that there is a decrease in the number of morphologically docked vesicles seen in *syt* mutants. The decreases in docking and evoked release are independent of the increase in spontaneous release. These results support the hypothesis that synaptotagmin stabilizes the docked state.

Key words: synaptic vesicles; Drosophila*;* synaptotagmin*; electron microscopy; vesicle docking; vesicle recycling*

To account for the rapidity of synaptic transmission, it has been proposed that a subset of synaptic vesicles in nerve terminals is docked at active zones where they form a pool that is readily releasable by an action potential. Electron microscopy of terminals has revealed a population of synaptic vesicles immediately adjacent to the presynaptic membrane (Couteaux and Pecot-Dechavassine, 1973). At least a portion of these morphologically docked vesicles is likely to correspond to the physiologically docked, fusion-ready pool.

Biochemical experiments have implicated the vesicle protein synaptotagmin in several aspects of nerve terminal function, including Ca^{2+} sensing (Brose et al., 1992; Chapman et al., 1995; Sutton et al., 1995; Shao et al., 1996, 1997) and endocytosis (Zhang et al., 1994; Jorgensen et al., 1995). In addition, synaptotagmin may participate in vesicle docking (Petrenko et al., 1991; Bennett et al., 1992; Sollner et al., 1993). Synaptotagmin contains two C2 repeats (Perin et al., 1990; Wendland et al., 1991), and homologous motifs occur in protein kinase C and cytosolic phospholipase A2, where they are thought to mediate a Ca^{2+}-dependent translocation of these enzymes to membranes (Clark et al., 1991). Several presynaptic membrane proteins bind synaptotagmin *in vitro*, including syntaxin, SNAP-25, neurexins, and the receptors for activated protein kinase C (Petrenko et al., 1991; Bennett et al., 1992; Mochly et al., 1992; Schiavo et al., 1997). These interactions may recruit vesicles to the release site in a manner analogous to the translocation of other C2 domain-containing proteins.

Recent genetic and pharmacological studies provide direct support for an involvement of synaptotagmin in neurosecretion (Bommert et al., 1993; Elferink et al., 1993), but they also suggest that synaptotagmin may not be essential for synaptic transmission. *Drosophila* larvae and *Caenorhabditis elegans* that lack the synaptotagmin (*syt*) gene are sluggish and uncoordinated yet are able to crawl and feed (DiAntonio et al., 1993b; Littleton et al., 1993b; Nonet et al., 1993). Evoked transmitter release is reduced to ~10% of control at the neuromuscular junctions of *Drosophila* syt^{null} mutants while spontaneous vesicle release is increased (Broadie et al., 1994). Similar reductions in Ca^{2+}-stimulated release are seen in hippocampal cultures from mice with altered synaptotagmin I (Geppert et al., 1994).

A decrease in evoked transmitter release could arise from several possible defects individually or in combination: a decrease in the number of docked vesicles, a decrease in the efficacy of Ca^{2+}-sensing or fusion, or an overall decrease in the number of vesicles. Two of these possibilities, an overall decrease in vesicles and a decrease in docked vesicles, can be addressed by a morphological examination. In the present study CNS synapses as well as a defined neuromuscular synapse were analyzed by light and electron microscopy in *Drosophila syt* mutants. The decrease in the number of morphologically docked vesicles that we observed

Received May 27, 1998; revised July 14, 1998; accepted July 16, 1998.

This work was supported by a Silvio Conte Center for Neuroscience Award from the National Institute of Mental Health (T.L.S.) and two grants from the Muscular Dystrophy Association (T.L.S. and N.E.R.). We are grateful to Drs. M. Ramaswami and E. Buchner for antibodies to CSP and to Ms. Fran Thomas for technical assistance.

Correspondence should be addressed to Dr. Thomas L. Schwarz at the above address.

in the absence of synaptotagmin supports the hypothesis that synaptotagmin stabilizes the docked state of vesicles at release sites.

MATERIALS AND METHODS

Genetics. Four *synaptotagmin* mutant lines were used for analysis. syt^{AD4} is a null mutation with a stop codon at amino acid 32. This mutant will be referred to as syt^{null}. syt^{AD3} is a hypomorph with a Y to N mutation at amino acid 364 (DiAntonio and Schwarz, 1994). $*,syt^{AD3}$ and $*,syt^{null}$ are chromosomes on which the *syt* alleles were placed in a different genetic background. These chromosomes were generated by homologous recombination between a second chromosome bearing one of the *syt* mutations (syt^{null} or syt^{AD3} chromosomes) and one bearing a P-element (P[HsGal4]). When the P-element containing portion of these recombined chromosomes is made homozygous, the increase in spontaneous transmitter release normally seen in *syt* mutants is suppressed (see Results). It is possible that the change in spontaneous release frequency is attributable to a novel mutation caused by the insertion of this P-element. Indeed, when the P-element containing parent chromosome (without any *syt* mutations) is made homozygous, the flies are uncoordinated (our unpublished observation). However, it is also possible that these changes could be caused by more complicated multigenic factors located on the chromosome bearing the P-element. Therefore, we will refer to this recombinant P-element-bearing second chromosome simply as *. Oregon R (*OrR*) larvae were used for wild-type controls.

To collect null mutants for fixation, we out-crossed females (syt^{null}/*Gla,Bc*) to *OrR* (+/+) males. syt^{null}/+ siblings were collected and crossed, and homozygous mutant (syt^{null}/syt^{null}) first instar larvae were selected on the basis of delayed hatching and sluggish behavior (DiAntonio et al., 1993b). syt^{AD3}/syt^{null} heterozygous larvae also were examined. These were generated by crossing syt^{AD3}/+ by syt^{null}/+ and selecting as above. The third and fourth *syt* mutations also were studied as heterozygotes ($*,syt^{AD3}/*,syt^{null}$ and $*,syt^{AD3}/syt^{null}$). These were generated by crossing $*,syt^{AD3}$/*Gla,Bc* by $*,syt^{null}$/*Gla,Bc* or by syt^{null}/*Gla,Bc* and selecting third instar larvae lacking *Bc*. An independent mutant line, $In(2)syt^{D27}$, which is also a null for *syt* (DiAntonio et al., 1993b), had a qualitatively similar phenotype.

Immunohistochemistry. Larvae were glued (Nexaband, Burns Veterinary Supply, Farmer's Branch, TX) to Sylgard-coated dishes containing cold Ca^{2+}-free Fly Ringer's solution (Jan and Jan, 1976). The cuticle was dissected open with a glass needle, the gut was removed, and the larvae were fixed in 1% formaldehyde in PBS for 15 min. They were rinsed briefly in PBS containing 0.1% Triton X-100 (PBST) and incubated overnight at 4°C in DCSP-1 [a monoclonal antibody directed against *Drosophila* cysteine string protein (Zinsmaier et al., 1994)] or a polyclonal rabbit antibody directed against horseradish peroxidase (HRP; ICN Biochemicals, Costa Mesa, CA) diluted 1:100 in dilution medium (PBST containing 10% normal goat serum). They were washed in PBST for 3 hr, incubated for 1 hr in a fluoresceinated secondary antibody (ICN Biochemicals), washed in PBST for 1 hr, and mounted in Citiflur AF-1 (City University, London, UK). For DCSP-1 experiments the CNS in whole mounts of first instar larvae were photographed on a Zeiss Axiophot microscope (Oberkochen, Germany). For anti-HRP experiments the synaptic boutons were counted on muscle fiber number 6 from abdominal segments 2–5 of third instar larvae (38 fibers from five animals for $*,syt^{AD3}/*,syt^{null}$ and 34 fibers from five animals for wild-type).

Electron microscopy. Dissected larvae were transferred immediately to cold primary fixative (1% acrolein and 2.5% glutaraldehyde in 0.1 M cacodylate buffer, pH 7.1) for 30–60 min. They were post-fixed in 1% osmium tetroxide in 0.1 M cacodylate for 1 hr, embedded in 1.5% agar to facilitate handling, dehydrated, and embedded in Embed 812 (Electron Microscopy Sciences, Fort Washington, PA). The 70 nm sections were stained with uranyl acetate and Sato's lead (Sato, 1967). For first instar larvae a section was cut at a random orientation approximately through the center of a larval brain hemisphere. The entire neuropil of this cross section was photographed at 12,000× magnification in the electron microscope for each of 10 larvae (three syt^{null}, three syt^{AD3}/syt^{null}, and four wild-type). For third instar larvae, sections through the region of neuromuscular junctions on muscle fiber number 6 from abdominal segments 2–5 were collected from each of six larvae (three $*,syt^{AD3}/*,syt^{null}$ and three wild-type). Electron micrographs covering the junctional region were taken at 12,000× magnification.

Image analysis. Control and experimental electron micrographs were printed together at the same magnification (3×) and then were coded and randomized for blind analysis. In each experiment the micrographs from a mutant larva were randomized with micrographs from a wild-type larva. However, both mutants were not always in each experiment; therefore, more wild-type synapses and larvae were used. Random synapses from widespread regions of first instar larval CNS were selected for analysis by using an adaptation of standard morphometric search protocols (Weibel, 1979). Each micrograph was overlaid with a grid pattern and was sampled systematically (in a spiral pattern) for synapses that had clear pre- and postsynaptic membranes. To avoid weighting the measurements in any given brain region, we included no more than five synapses per micrograph in the analysis. The first five synapses encountered in the grid pattern that fit the search criteria (i.e., clear pre- and postsynaptic membranes) were marked, regardless of the number of synapses per terminal or the number of synapses per micrograph. This morphometric search protocol usually resulted in only one synapse per terminal being marked; however, the protocol occasionally yielded two synapses in a given terminal. For analysis of vesicle distributions the individual synapses were magnified (~3×) through a video camera, and the images were captured onto a Macintosh computer. The total numbers of synapses analyzed were 231 for wild-type (from four larvae), 154 for syt^{null} (from three larvae), and 122 for syt^{AD3}/syt^{null} (from three larvae).

The presynaptic membrane, as determined by the extent of the synaptic cleft, was marked in these cross sections (e.g., Fig. 2*B*) and measured with either an Image 1 analysis system (Universal Imaging, West Chester, PA) or National Institutes of Health Image software (Bethesda, MD). The shortest distance from the presynaptic membrane to the center of each vesicle was measured (e.g., Fig. 2*B*). To avoid the inclusion of vesicles located closer to a neighboring synapse, we included only vesicles within 200 nm of the presynaptic membrane in the quantification. Almost all vesicles in the small category were clear and 30 nm in diameter, which is typical of small clear synaptic vesicles in *Drosophila* (Budnik et al., 1990). The large vesicle category was much more heterogeneous; vesicle diameters ranged from 45 to ~90 nm, and some were opaque. Microtubules cut transversely occasionally may resemble a vesicular structure; however, their small diameter [~20 nm (Peters et al., 1991)] permitted unequivocal exclusion from this study.

To assess the distribution of small clear synaptic vesicles with respect to the presynaptic membrane, we sorted CNS distance data into 6 nm bins. The mean number of vesicles per synapse was graphed versus distance from the presynaptic membrane (see Fig. 5*A*). Because small clear synaptic vesicles have a radius of 15 nm, we have defined the morphologically docked pool as those vesicles for which the centers are 12–18 nm from the presynaptic membrane.

Similar measurements were made on third instar neuromuscular junctions, with a few modifications. After coding and randomizing mutant and wild-type micrographs, we marked neuromuscular junctions with clear pre- and postsynaptic membranes and at least one presynaptic dense body. Images were imported into National Institutes of Health Image software, as described above. To assess the distribution of vesicles in the vicinity of active zones, we marked 100 nm of presynaptic membrane on either side of a presynaptic dense body. Then the perpendicular distance from the marked presynaptic membrane to the center of each vesicle within 200 nm was measured (see Fig. 8*B*). Because the presynaptic membrane of sectioned third instar larval neuromuscular junctions often extends several hundreds of nanometers beyond active zones, the measurements were restricted to vesicles directly above the marked region of the presynaptic membrane (i.e., near active zones). The total number of synapses analyzed was 91 for wild-type (from three larvae) and 106 for $*,syt^{AD3}/*,syt^{null}$ (from three larvae).

Electrophysiology. Intracellular voltage recordings were made from body wall muscle 6 from abdominal segments 4 or 5 of third instar larvae according to the procedures of Stewart and colleagues (Stewart et al., 1994), except that stocks used for the recordings were maintained at 18°C. Larvae were dissected and recorded in HL3 Ringer's solution [containing (in mM) 70 NaCl, 5 KCl, 1.5 $CaCl_2$, 20 $MgCl_2$, 10 $NaHCO_3$, 5 trehalose, 115 sucrose, and 5 HEPES, pH 7.2]. Four fibers from $*,syt^{AD3}/*,syt^{null}$ larvae, 10 fibers from $*,syt^{AD3}/syt^{null}$ larvae, and six fibers from wild-type larvae were analyzed; only one fiber per larva was used. The CNS was removed by sectioning the nerves near the ventral ganglion. For evoked potentials the nerve end was stimulated by using a heat-polished suction electrode. Mean miniature excitatory junction potential (mEJP) frequency was calculated from data that were collected for ~2 min.

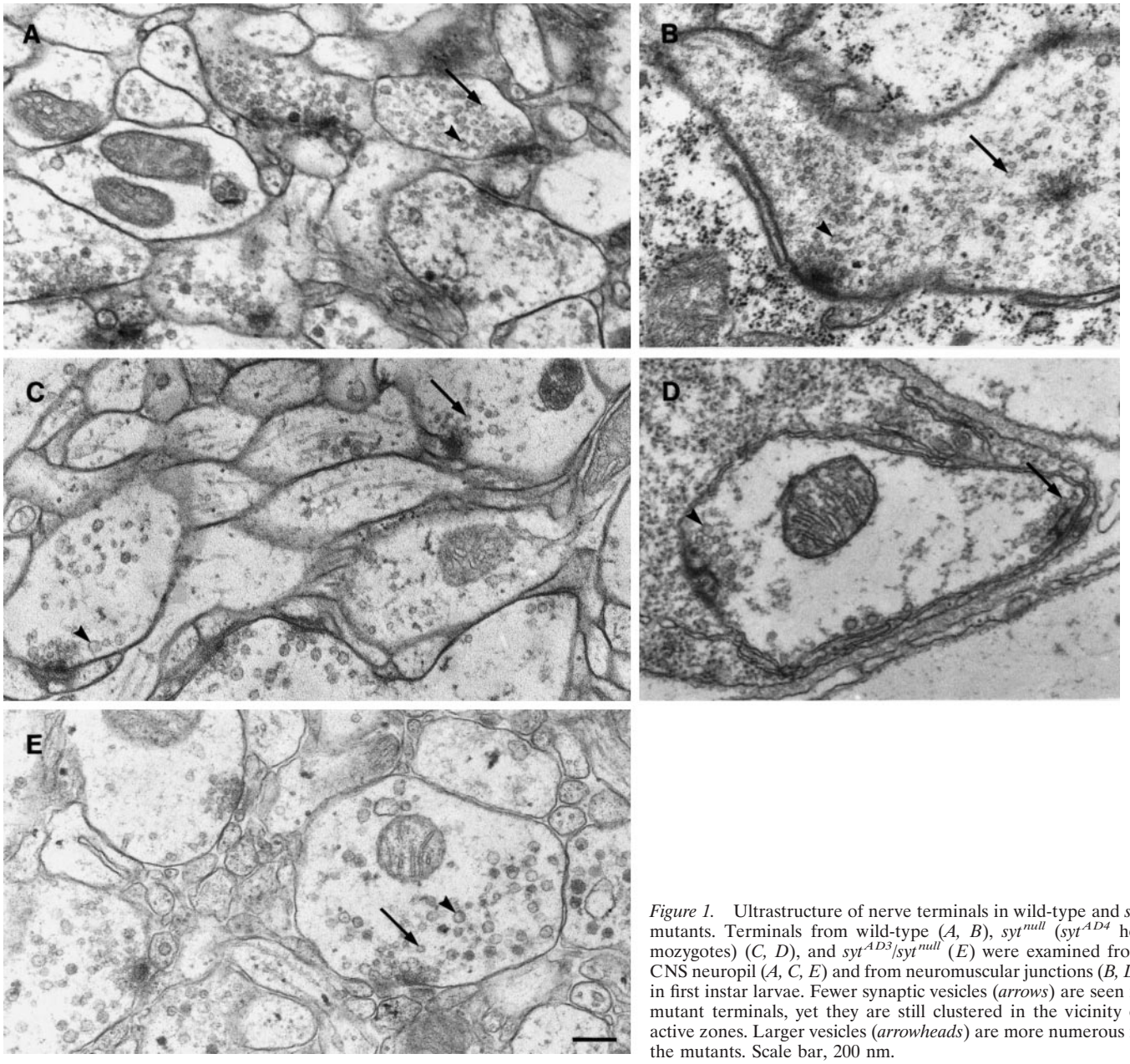

Figure 1. Ultrastructure of nerve terminals in wild-type and *syt* mutants. Terminals from wild-type (*A, B*), syt^{null} (syt^{AD4} homozygotes) (*C, D*), and syt^{AD3}/syt^{null} (*E*) were examined from CNS neuropil (*A, C, E*) and from neuromuscular junctions (*B, D*) in first instar larvae. Fewer synaptic vesicles (*arrows*) are seen in mutant terminals, yet they are still clustered in the vicinity of active zones. Larger vesicles (*arrowheads*) are more numerous in the mutants. Scale bar, 200 nm.

RESULTS

Vesicles are targeted to and clustered at synapses in *syt* mutants

Two *Drosophila* lines carrying mutations in the *synaptotagmin* gene (DiAntonio et al., 1993b; DiAntonio and Schwarz, 1994) were analyzed. syt^{AD4}, which will be referred to simply as syt^{null}, produces no synaptotagmin protein (see Materials and Methods) and is homozygous-lethal. syt^{AD3} is a point mutant with a single altered amino acid in its second C2 domain. This allele has a less severe phenotype and permits a few mutants to survive to adulthood when it is placed over a deficiency that removes *syt* ($syt^{AD3}/Df\ (2L)DTD2$). In the present study we used larvae that were either syt^{null} homozygotes or, a less severe allelic combination, syt^{AD3}/syt^{null} heterozygotes.

Synapses were examined by electron microscopy in first instar larvae, the last stage at which viable larvae can be collected for the null alleles. Immunocytochemistry has demonstrated that the *syt* product is located both at CNS synapses and neuromuscular junctions (DiAntonio et al., 1993b; Broadie et al., 1994). To obtain a large number of nerve terminals for quantitative analysis, we used random sections through larval brain hemispheres (Fig. 1*A,C,E*; see Materials and Methods). Neuromuscular junctions also were examined in wild-type (Fig. 1*B*) and syt^{null} (Fig. 1*D*) first instar larvae. Qualitatively, neuromuscular junctions showed the same phenotype as the central synapses of first instar larvae (see below).

To analyze CNS synapses, we adopted sampling procedures (see Materials and Methods) to insure a diverse population of synapses in each sample so that general and robust changes in vesicle distribution could be assessed. Large numbers of synapses from widespread regions of brain hemisphere neuropil were examined for each genotype. Synaptotagmin is expressed throughout the neuropil and is believed to be important for synaptic transmission at all or most synapses (DiAntonio et al., 1993a;

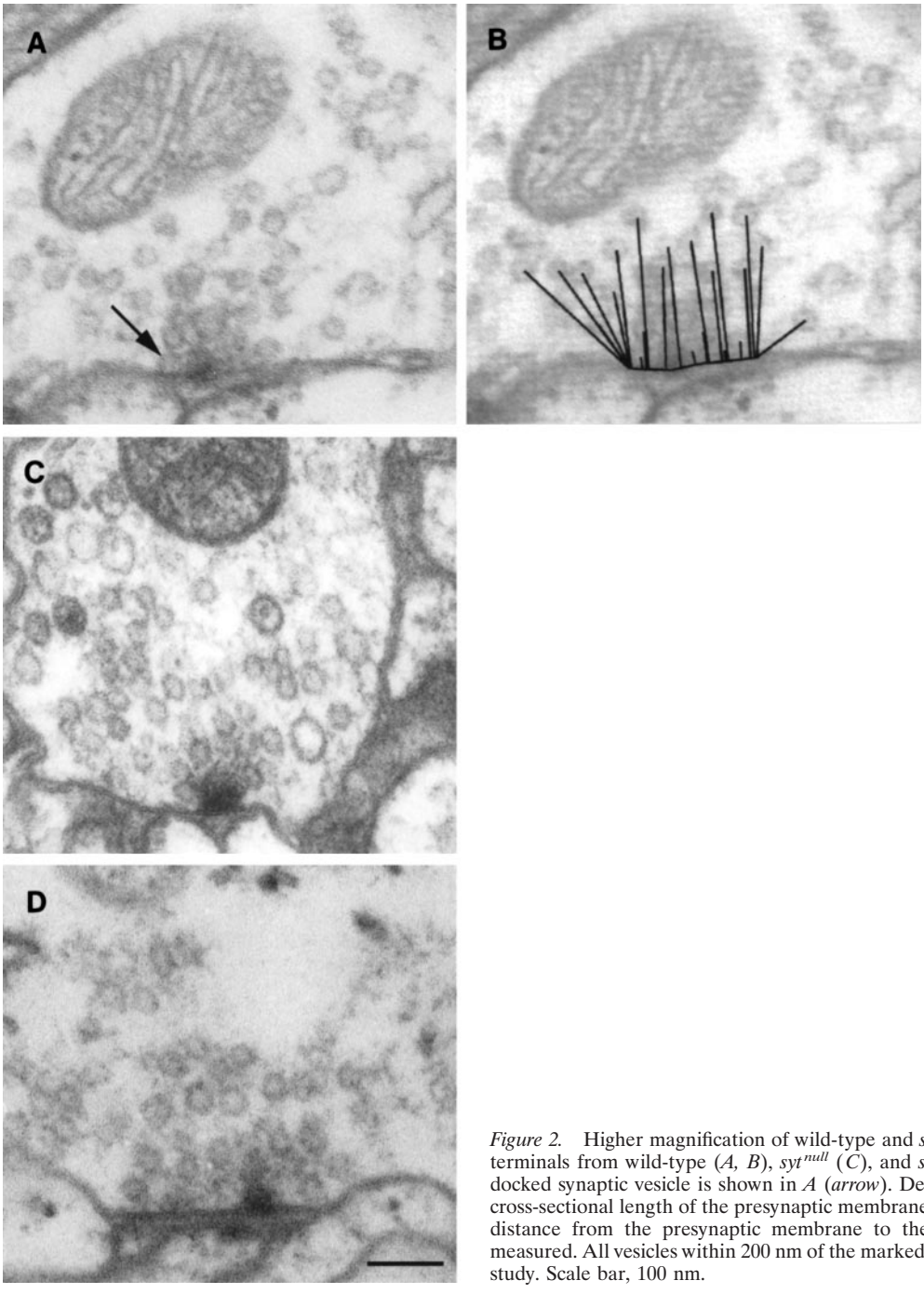

Figure 2. Higher magnification of wild-type and *syt* mutant nerve terminals. Shown are CNS terminals from wild-type (*A, B*), syt^{null} (*C*), and syt^{AD3}/syt^{null} (*D*) larvae. A morphologically docked synaptic vesicle is shown in *A* (*arrow*). Details of measurements are shown in *B*. The cross-sectional length of the presynaptic membrane was measured at each synapse. The closest distance from the presynaptic membrane to the center of each vesicle was marked and measured. All vesicles within 200 nm of the marked presynaptic membrane were included in the study. Scale bar, 100 nm.

Littleton et al., 1993a; Broadie et al., 1994; DiAntonio and Schwarz, 1994). Thus a role in a fundamental process such as vesicle docking would be expected to be manifest in the general population of synapses. For each mutant specimen that was examined, a wild-type control was sectioned and analyzed in parallel. As shown below, there was some variability in the observed morphological parameters from sample to sample. In part, this may be attributable to differences in the subsets of synaptic types that fell into a given sample. However, this variation proved small in comparison to the differences between genotypes. Thus, whether parameters were compared for each individual mutant specimen and its paired wild-type control (as in Fig. 6) or by pooling all of the data for a genotype (as in Figs. 3, 5, 7, 9), robust and statistically significant changes were detected that were attributable to the mutations.

syt mutants of both genotypes had a generally normal ultrastructure (Budnik et al., 1990): conventional presynaptic membrane specializations were observed, each with clear 30 nm synaptic vesicles clustered nearby, as in wild-type larvae (Figs. 1, 2). However, there were some distinct differences in the vesicle populations. Nerve terminals from syt^{null} mutants contained fewer 30 nm synaptic vesicles (*arrow*, compare Fig. 1*C,D* with *A,B*; see also Fig. 3). This change was most dramatic in regions of the terminal that were distant from synaptic sites; few vesicles in mutant terminals were observed outside tight clusters near synapses (see Fig. 1*C–E*). In addition, larger heterogeneous vesicles

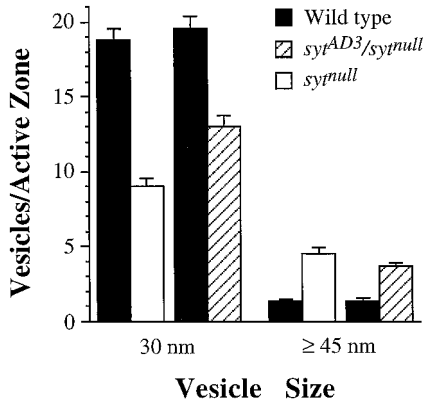

Figure 3. Number of vesicles within 200 nm of the presynaptic membrane. Normal 30 nm synaptic vesicles are depleted, whereas large irregularly shaped vesicles are enriched at CNS synapses from *syt* mutants; the effect is strongest in the null allele. Mutants are graphed versus their paired wild-type control: 154 syt^{null} synapses versus 161 wild-type; 122 syt^{AD3}/syt^{null} synapses versus 118 wild-type. The values graphed are the means ± SEM ($p \ll 0.001$ for each pair; Student's *t* test).

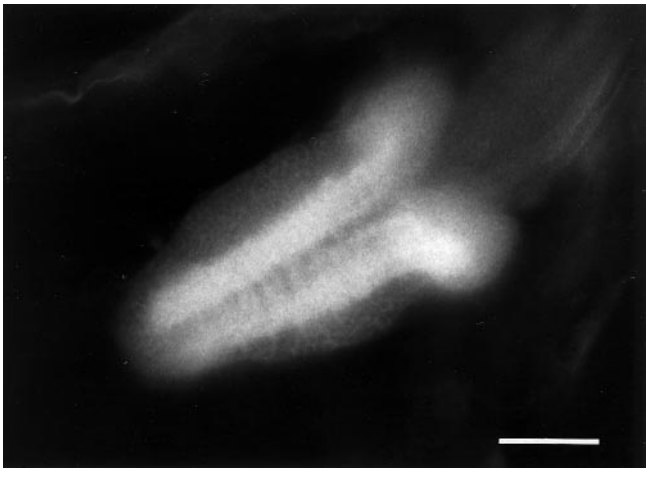

Figure 4. Cysteine string protein in the CNS of a syt^{null} mutant is highly concentrated in the neuropil. First instar larvae of syt^{null} mutants were labeled with a monoclonal antibody directed against the vesicle-associated cysteine string protein, followed by fluorescein-conjugated goat anti-mouse IgG. The bright staining is located in the neuropil of the ventral nerve cord and the brain hemispheres (which are not in the plane of focus). Faint staining was also visible in the cell body layer. Scale bar, 100 μm.

were more abundant in the mutants (Figs. 1*C–E, arrowhead*; 3). The large vesicles were not concentrated near active zones. syt^{AD3}/syt^{null} had an intermediate phenotype with a less dramatic decrease in the number of synaptic vesicles (Figs. 1*E, arrow*; 3) and an intermediate number of large vesicles (Figs. 1*E, arrowhead*; 3).

To quantify the changes at mutant synapses, we counted vesicles within 200 nm of the presynaptic membrane. Because the morphological properties of individual synapses within the CNS were quite variable, a blind morphometric analysis of large numbers of randomly selected synapses was conducted to determine the average properties in each genotype (see Materials and Methods). Vesicles were categorized as either small clear synaptic vesicles (<45 nm in diameter) or large vesicles (≥45 nm in diameter). The number of synaptic vesicles per synapse in syt^{null} homozygotes and syt^{AD3}/syt^{null} was decreased to 48 and 66% of wild-type, respectively (Fig. 3). In contrast, large vesicles were 3.4-fold and 2.6-fold more abundant in syt^{null} and syt^{AD3}/syt^{null} mutants, respectively (Fig. 3).

The decrease in synaptic vesicles observed in the mutant terminals raised the possibility that vesicles might not be targeted correctly in the mutants. For example, mutant vesicles might accumulate in the cell body because of inefficient transport down the axon, as seen in kinesin mutants (Hall and Hedgecock, 1991). A brief examination of the surrounding neuronal cell body layer, in sections in which the central neuropil was analyzed extensively, showed no obvious accumulations of 30 nm vesicles ($n > 30$ somas; data not shown). To investigate the overall distribution of vesicles more thoroughly, we examined the distribution of another synaptic vesicle-associated protein, cysteine string protein (CSP; Mastrogiacomo et al., 1994; Zinsmaier et al., 1994), by immunocytochemistry. As in control animals (data not shown), CSP staining in the nervous system of syt^{null} mutants is highly concentrated in the neuropil, with minor staining in the cell body regions (Fig. 4). Thus, synaptic vesicles appear to be targeted correctly to nerve terminals in the *syt* mutants.

The number of morphologically docked vesicles is reduced in *syt* mutants

The nerve terminal may be viewed as containing distinct pools of synaptic vesicles: synaptic vesicles that are not obviously associated with a synapse, synaptic vesicles that are clustered in the vicinity of a synapse, and synaptic vesicles that are immediately adjacent to the presynaptic membrane, which we define as morphologically docked (see Fig. 2*A, arrow*; see also Materials and Methods). Although this last pool may include vesicles that are adjacent to the membrane at a synapse by chance, without being functionally docked, this pool also must include the docked vesicles (Couteaux and Pecot-Dechavassine, 1973; Koenig et al., 1993). Indeed, the morphological assessment of the docked state of vesicles has been used in numerous investigations of synaptic mechanisms (Bommert et al., 1993; Hunt et al., 1994; Broadie et al., 1995; O'Connor et al., 1997). By examining the distribution of synaptic vesicles relative to the presynaptic membrane, we have determined that the reduction in vesicle number is not uniform throughout the terminal. In particular, as described below, the pool of morphologically docked vesicles is reduced more sharply than the pool of vesicles clustered in the close vicinity of the synapse.

For this analysis we marked the extent of the presynaptic membrane and measured the distance from the center of each vesicle to the nearest point of the presynaptic membrane (see Fig. 2*B*). The data were pooled into 6 nm bins (Fig. 5*A*). The bin of vesicles for which the centers were 12–18 nm (one radius ± 3 nm) from the presynaptic membrane was defined as the morphologically docked pool. Because the area in each bin generally increases with increasing distance from the presynaptic membrane (see Fig. 2*B*), equal numbers of vesicles per bin actually reflect a decrease in vesicle density away from the synapse. To facilitate the comparison between the *syt* mutant and control terminals, we graphed the data for the mutants as a percentage of control (Fig. 5*B*). The observed reduction in synaptic vesicles was not uniform across this region. Although *syt* mutants had fewer 30 nm synaptic vesicles than controls, the vesicles nevertheless were clustered tightly in the vicinity of synapses. In the mutants the pools of vesicles 18–50 nm from the presynaptic membrane showed the least attenuation. Here, both *syt* mutants had ~75% of the control number of vesicles. Despite this relative accumulation of vesicles

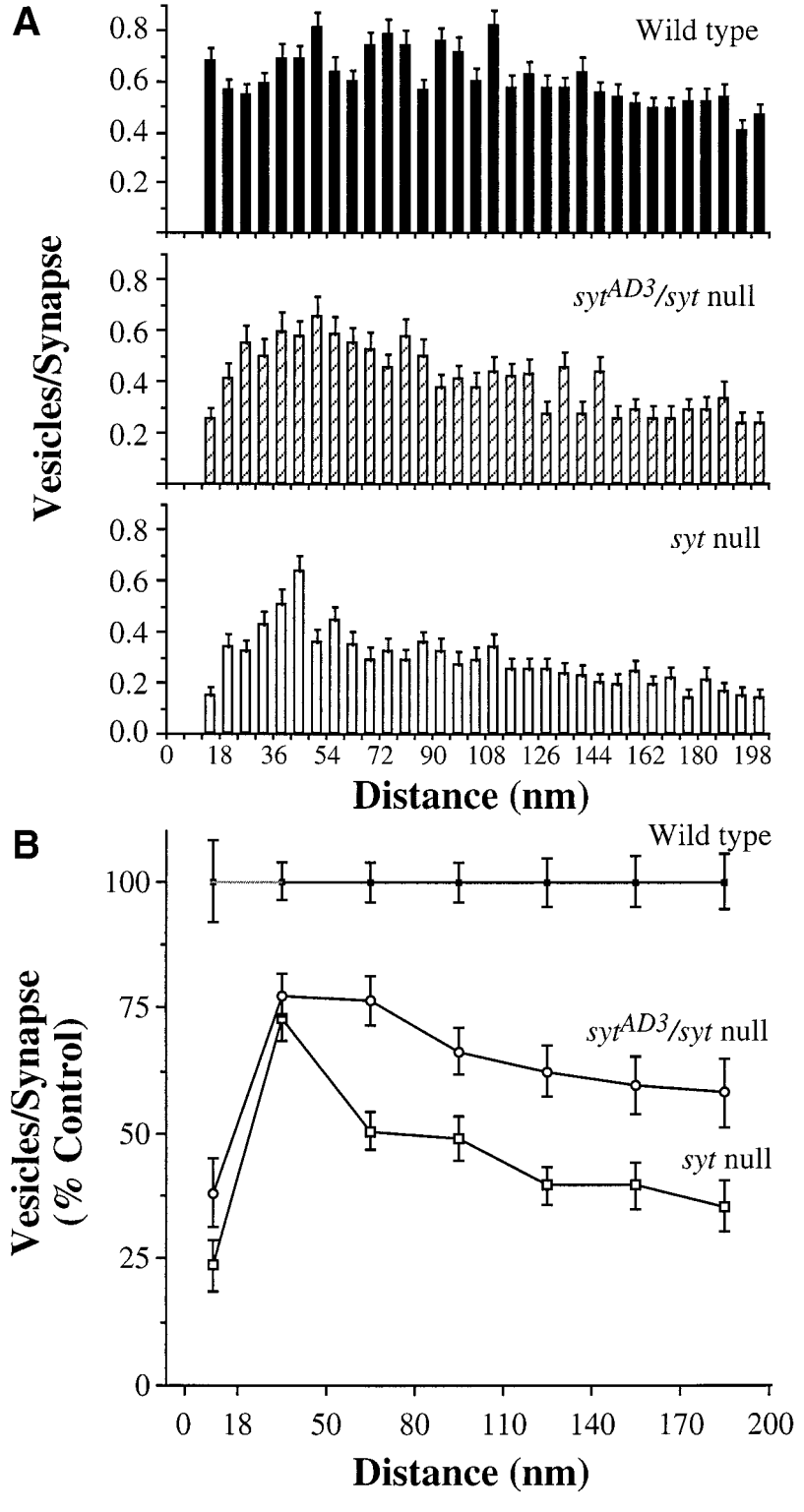

Figure 5. Distribution of synaptic vesicles within 200 nm of the presynaptic membrane in neuropil. The distance of vesicles from the presynaptic membrane was determined in each genotype (see Fig. 2*B* and Materials and Methods), and a histogram of their distribution is shown (*A*; means ± SEM). The total number of synapses analyzed was: wild-type, 231; syt^{null}, 154; and syt^{AD3}/syt^{null}, 122. For a comparison of the vesicle population at each distance, the data from each mutant genotype were plotted as a percentage of its paired wild-type control (*B*; syt^{null}, $n = 154$ vs wild-type $n = 161$; syt^{AD3}/syt^{null}, $n = 122$ vs wild-type $n = 118$; means ± SEM). Each of the mutant values was statistically significantly different from its paired control ($p \ll 0.001$; except the 50–80 nm bin of syt^{AD3}/syt^{null}; $p < 0.01$; Student's *t* test). The 12–18 nm bin, which is likely to represent morphologically docked vesicles, was kept separate, whereas the rest of the bins were enlarged to one vesicle diameter, 30 nm, to reduce random scatter. The number of morphologically docked vesicles is markedly reduced in *syt* mutants although vesicles are clustered nearby at levels approaching wild-type levels.

nearby, in the *syt* mutants the number of 30 nm vesicles immediately adjacent to the presynaptic membrane was reduced markedly: to 24% of control in syt^{null} homozygotes and to 38% in syt^{AD3}/syt^{null}.

The dramatic decrease in the number of morphologically docked vesicles was a consistent finding that could not have resulted from the chance selection of atypical regions in individual specimens and a consequent distortion of the mean. To illustrate this point, in Figure 6 we have graphed the mean number of morphologically docked vesicles per synapse for each individual mutant that was analyzed and paired it with the control specimen from the same blind experiment. In every pair the number of morphologically docked vesicles was reduced significantly in the *synaptotagmin* mutant relative to its wild-type control (p values ranged from $p < 0.02$ to $\ll 0.001$; Student's *t* test). Although variation naturally was encountered from synapse to

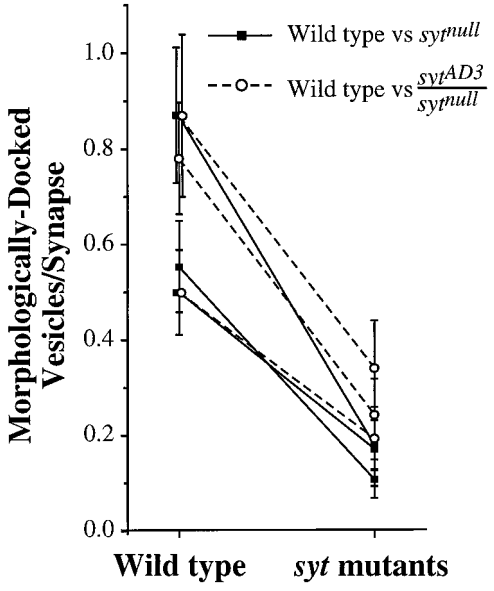

Figure 6. The number of morphologically docked vesicles was reduced in every mutant larva that was examined. The mean number of morphologically docked vesicles per synapse ± SEM is graphed for each pair of simultaneously analyzed larvae (for all three larvae in one experiment in which a single wild-type and both syt^{null} and syt^{AD3}/syt^{null} were analyzed in parallel). The decrease in morphological docking was statistically significant for each set that was analyzed (p values ranged from < 0.02 to $\ll 0.001$; Student's t test).

synapse and from data set to data set, the trend was consistent and the change in the mean for each genotype was statistically different from control at $p \ll 0.001$ (see Fig. 5*B*). Thus, our methods for collecting large amounts of data from widespread regions of a single randomly oriented cross section through a brain hemisphere succeeded in identifying a widespread and dramatic change in vesicle docking that far exceeded the normal variation from sample to sample.

The mean cross-sectional length of the presynaptic membrane in these sections was not altered substantially in the mutants: wild-type, 177 ± 5 nm; syt^{null}, 169 ± 5 nm; syt^{AD3}/syt^{null}, 196 ± 6 nm (length ± SEM). To determine whether these slight differences in mean cross-sectional presynaptic length between individual larvae significantly influenced the docking data, we normalized the number of morphologically docked vesicles per synapse to the mean length of presynaptic membrane in each larva. As shown in Table 1, the mean number of morphologically docked vesicles per micrometer of presynaptic membrane was not significantly different between individual larvae within each genotype (wild-type, $p < 0.2$; syt^{null}, $p < 0.6$; syt^{AD3}/syt^{null}, $p < 0.3$; ANOVA), yet the mean number of morphologically docked vesicles per micrometer of presynaptic membrane was reduced to 25% of control in syt^{null} ($p \ll 0.0001$; ANOVA) and 37% of control in syt^{AD3}/syt^{null} ($p \ll 0.0001$; ANOVA). Thus, along with the decrease in morphological docking per synapse, there was a decrease in docking per unit length of presynaptic membrane.

The decrease in docking occurs at neuromuscular junctions and is independent of the increase in spontaneous release

To determine whether the decrease in the number of morphologically docked vesicles in the *syt* mutants was secondary to the increased frequency of spontaneous release, we examined the mutant genotype $*,syt^{AD3}/*,syt^{null}$. This genotype suppresses the increased rate of spontaneous release normally seen in *syt* mutants. The **,syt* chromosomes were created by homologous recombination events that changed the genetic background of the second chromosome (see Materials and Methods). The basis of this change has not yet been characterized; it may be attributable to simple disruption of a novel gene by the P-element located on the * chromosome or to a more complex multigenic effect (see Materials and Methods). Because the $*,syt^{AD3}/*,syt^{null}$ mutants survive to the third instar larval stage, both the physiological measurements and the morphological measurements were done at the third instar neuromuscular junction of muscle fiber number 6. $*,syt^{AD3}/*,syt^{null}$ exhibited the expected decrease in evoked transmitter release (Fig. 7*A*). However, the increased rate of spontaneous transmitter release usually seen in *syt* mutants was suppressed in this genotype; the rate of spontaneous release now remained the same as control (Fig. 7*B*; $p < 0.8$; Student's t test). On the other hand, $*,syt^{AD3}/syt^{null}$ exhibited the expected increased rate of spontaneous release (Fig. 7*B*; $p \ll 0.001$; Student's t test). Thus, this suppression of the increased rate of spontaneous release was seen only in larvae that were homozygous for the uncharacterized portion (*) of the second chromosome (see Materials and Methods).

The decreased rate of spontaneous release in this genotype could arise from a decreased probability of release at the synapse or from a decrease in the number of synapses on the muscle fiber. To address the latter possibility, we counted the number of boutons on muscle fiber number 6 in anti-HRP-stained preparations of $*,syt^{AD3}/*,syt^{null}$ and wild-type. There was no statistically significant difference in the number of boutons per muscle fiber: mutants had 58.7 ± 4.1 (34 fibers from six animals), whereas wild-type had 53.1 ± 3.2 (38 fibers from six animals; mean number of boutons per fiber ± SEM; $p < 0.3$; Student's t test).

To determine the effect of this change in genetic background on vesicle populations and vesicle distribution, we examined the ultrastructure of third instar neuromuscular junctions on muscle fiber number 6 (Fig. 8). The distribution of synaptic vesicles with respect to the presynaptic membrane was determined as described above, with a few modifications. The presynaptic membrane at neuromuscular junctions of third instar larvae was often >1 μm in length. To restrict the analysis to the vicinity of active zones, we marked off 100 nm of presynaptic membrane on each side of the dense body of the active zone. Then the perpendicular distance from the center of each synaptic vesicle to this marked region of the presynaptic membrane was measured (Fig. 8*B*). All of the vesicles within 200 nm perpendicular to this region of presynaptic membrane were included in the analysis.

We found that the overall number of synaptic vesicles near active zones in the $*,syt^{AD3}/*,syt^{null}$ mutants is increased slightly as compared with control (Fig. 9*A*; $p < 0.01$; Student's t test). This increase in $*,syt^{AD3}/*,syt^{null}$ is in direct contrast to the overall reduction in the number of synaptic vesicles near synapses in the two *synaptotagmin* mutants (syt^{null} and syt^{AD3}/syt^{null}) that exhibit an increased frequency of spontaneous release (Broadie et al., 1994; DiAntonio and Schwarz, 1994). The inverse correlation between vesicle number and spontaneous release frequency suggests that the overall number of vesicles near synapses may be influenced by the rate of spontaneous release.

The number of large vesicles near active zones in the $*,syt^{AD3}/*,syt^{null}$ mutants also is increased as compared with wild-type (Fig. 9*A*), similar to the changes in the other two mutants (see Fig. 3). Thus, the changes in the small vesicle population in the

Table 1. Morphologically docked vesicles/μm presynaptic membrane

Genotype	Larva	Mean number of docked vesicles: Synapse	Mean cross-sectional length of presynaptic membrane (μm): Synapse	*Mean number of docked vesicles: Presynaptic membrane (μm)
Wild type	1 ($n = 74$)[a]	0.55 ± 0.1	0.160 ± 0.009	3.4 ± 0.6
	2 ($n = 39$)[a]	0.85 ± 0.1	0.184 ± 0.014	4.6 ± 0.8
	($n = 32$)[b]	0.78 ± 0.1	0.164 ± 0.011	4.7 ± 0.7
	3 ($n = 38$)[b]	0.87 ± 0.2	0.204 ± 0.013	4.3 ± 0.8
	4 ($n = 48$)[a,b]	0.50 ± 0.09	0.186 ± 0.009	2.7 ± 0.5
	1–4 ($n = 231$)	0.68 ± 0.05	0.177 ± 0.005	3.8 ± 0.3
	1, 2, 4 ($n = 161$)[a]	0.61 ± 0.06	0.174 ± 0.006	3.5 ± 0.4
	2, 3, 4 ($n = 118$)[b]	0.69 ± 0.07	0.186 ± 0.006	3.7 ± 0.4
syt^{null}	1 ($n = 64$)	0.11 ± 0.04	0.170 ± 0.010	0.65 ± 0.2
	2 ($n = 55$)	0.18 ± 0.05	0.178 ± 0.013	1.0 ± 0.3
	3 ($n = 35$)	0.17 ± 0.08	0.152 ± 0.010	1.1 ± 0.5
	1–3 ($n = 154$)	0.15 ± 0.03	0.169 ± 0.007	0.89 ± 0.2
syt^{AD3}/syt^{null}	1 ($n = 41$)	0.24 ± 0.08	0.227 ± 0.016	1.1 ± 0.3
	2 ($n = 35$)	0.34 ± 0.1	0.166 ± 0.009	2.0 ± 0.6
	3 ($n = 46$)	0.22 ± 0.07	0.189 ± 0.014	1.1 ± 0.4
	1–3 ($n = 122$)	0.26 ± 0.05	0.196 ± 0.008	1.4 ± 0.2

All values are mean ± SEM. The synapses from wild-type larva 2 were divided into two groups for analysis with each of the mutants separately. In one experiment, all three genotypes (wild-type larva 4, syt^{null} larva 3, and syt^{AD3}/syt^{null} larva 3) were analyzed in parallel.

[a]Wild-type synapses that were analyzed in parallel with syt^{null} synapses.

[b]Wild-type synapses that were analyzed in parallel with syt^{AD3}/syt^{null} synapses.

*The mean number of morphologically docked vesicles per micron of presynaptic membrane was not significantly different between individual larvae within each genotype (wild type, $p < 0.2$; syt^{null}, $p < 0.6$; syt^{AD3}/syt^{null}, $p < 0.3$; ANOVA). However, the mean number of morphologically docked vesicles per micron of presynaptic membrane was reduced to 25% of control in syt^{null} ($p \ll 0.0001$; ANOVA) and 37% of control in syt^{AD3}/syt^{null} ($p \ll 0.0001$, ANOVA; mutant synapses were compared only to wild-type synapses analyzed in parallel).

immediate vicinity of synapses do not correlate directly to the changes in the large vesicle population in this area.

To determine the number of morphologically docked vesicles in these mutants, we graphed the number of small vesicles per synaptic region versus the distance from the presynaptic membrane (Fig. 9*B*). Because only synaptic vesicles directly above the marked region were included, the area in each bin is generally constant regardless of distance from the membrane. In wild-type synapses it is apparent that the pool of vesicles immediately adjacent to the presynaptic membrane is quite enriched. Naturally, because these data were obtained from third instar neuromuscular junctions and not first instar central synapses, the proportion of docked vesicles is not directly comparable to those in Figure 5*A*. The data were regraphed as a percentage of control to aid comparison (Fig. 9*C*). Despite the slight increase in the overall number of synaptic vesicles near active zones (Fig. 9*A*), the number of morphologically docked vesicles is reduced markedly in these *syt* mutants to 33% of control (Fig. 9*C*; $p \ll 0.001$; Student's *t* test).

The results from the $*,syt^{AD3}/*,syt^{null}$ mutants demonstrate that the decrease in morphological docking (1) occurs at a defined peripheral synapse as well as at randomly sampled CNS synapses, (2) is independent of overall vesicle depletion, and (3) is independent of the increased rate of spontaneous vesicle fusions found in the other *syt* mutants.

DISCUSSION

We have conducted a morphometric analysis of the ultrastructural phenotype of synaptotagmin mutants. We are particularly interested in the subset of vesicles that are morphologically docked (i.e., immediately adjacent to the presynaptic membrane), because vesicles that are functionally docked are likely to be included in this pool (Couteaux and Pecot-Dechavassine, 1973; Bommert et al., 1993; Koenig et al., 1993; Hunt et al., 1994; Broadie et al., 1995; O'Connor et al., 1997). In the CNS those 30 nm vesicles for which the centers are located within 18 nm of the presynaptic membrane are defined as morphologically docked. At the neuromuscular junction the analysis was limited further to 100 nm of presynaptic membrane on either side of the dense body. Synapses from all of the *syt* mutants that were analyzed exhibited a dramatic decrease in morphologically docked vesicles: CNS synapses from syt^{null} mutants had 24% of the control, CNS synapses from syt^{AD3}/syt^{null} had 38% of the control, and neuromuscular junctions on muscle fiber number 6 from $*,syt^{AD3}/*,syt^{null}$ had 33% of the control number of morphologically docked vesicles per synapse.

Larval brain neuropil contains a heterogeneous mixture of synapses (Bate and Martinez Arias, 1993). Synaptotagmin is expressed throughout the neuropil and is thought to function at most, perhaps all, synapses (DiAntonio et al., 1993a; Littleton et al., 1993a; DiAntonio and Schwarz, 1994) although, naturally, synaptotagmin function has not been demonstrated at every synapse in the CNS. To minimize any sampling artifact caused by differences between individual CNS synapses or changes in active zone size, we took the following precautions during data collection and analysis: (1) We analyzed large numbers of randomly selected synapses (Weibel, 1979) from widespread regions of larval brain hemispheres and limited the number of synapses per micrograph included in the study to prevent synapses in any one

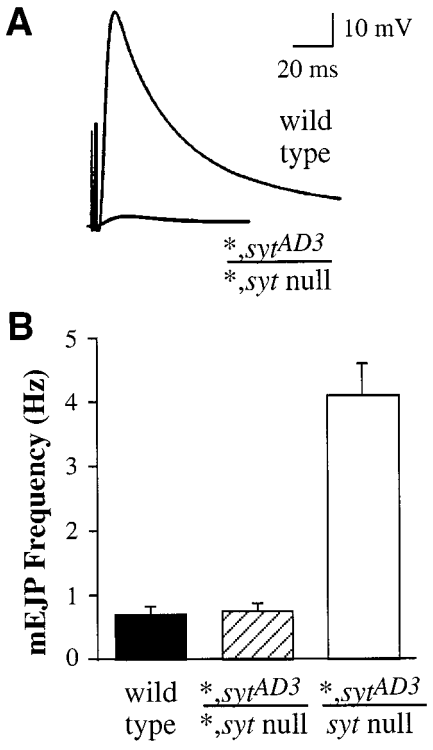

Figure 7. An altered genetic background (*; see Materials and Methods) reduces the frequency of spontaneous vesicle fusions to control levels in a *synaptotagmin* mutant. *A*, Representative traces of evoked EJPs recorded from wild-type and mutant (*$,syt^{AD3}$/*$,syt^{null}$) larvae. *B*, Mean mEJP frequency ± SEM is plotted for wild-type (*black bars*; $n = 6$), *$,syt^{AD3}$/*$,syt^{null}$ (*hatched bars*; $n = 4$), and *$,syt^{AD3}$/syt^{null} (*white bars*; $n = 10$) larvae. mEJP frequency was increased significantly as compared with wild-type in *$,syt^{AD3}$/syt^{null} mutants ($p \ll 0.001$; Student's *t* test), as seen previously in other *syt* mutations. This increase was suppressed when the portion of the second chromosome denoted * (see Materials and Methods) was made homozygous; mEJP frequency in this mutant (*$,syt^{AD3}$/*$,syt^{null}$) was not significantly different from wild-type larvae ($p < 0.8$; Student's *t* test).

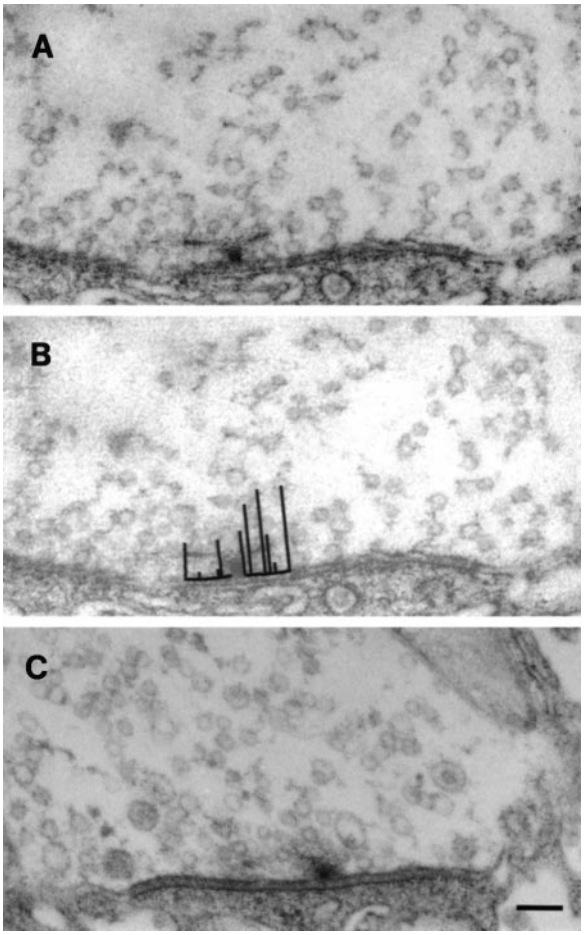

Figure 8. Third instar larval neuromuscular junctions from wild-type (*A, B*) and *$,syt^{AD3}$/*$,syt^{null}$ mutants (*C*). Vesicle distribution was measured in the vicinity of dense bodies. One hundred nanometers of presynaptic membrane was marked (*B*) on either side of the dense body. The perpendicular distance from the marked presynaptic membrane to the center of each vesicle was marked and measured. All vesicles within 200 nm perpendicular to the marked membrane were included in the study. Scale bar, 100 nm.

region from unduly influencing the mean (see Materials and Methods). (2) We conducted a pairwise comparison of each mutant larva to its simultaneously analyzed control and found the morphological changes to be universal (e.g., Fig. 6). A sampling artifact would require that all six mutant sections over-represent putative "low docking" areas, whereas all four wild-type sections over-represent putative "high docking" areas. Because each sample was independent and from a randomly oriented section, the differences we observed are attributable to the mutations. (3) We analyzed the number of morphologically docked vesicles per synapse (see Fig. 5) as well as the number per unit length of presynaptic membrane (see Table 1). (4) We included analysis of a defined synapse, the neuromuscular junction on muscle fiber number 6 (see Fig. 9). If the decrease in morphological docking at CNS synapses of *syt* mutants were an artifact of sampling or abnormal CNS development, then a similar decrease would not be expected near active zones of a specific neuromuscular junction.

We found that the mean number of morphologically docked vesicles at synapses in *syt* mutants was reduced dramatically in every case. Every pairwise comparison of CNS synapses from a *syt* mutant larva to its simultaneously analyzed wild-type control showed a decreased number of morphologically docked vesicles. When they were normalized per unit length of presynaptic membrane, *syt* mutants still exhibited a dramatic decrease in the mean number of morphologically docked vesicles as compared with wild-type ($p < 0.0001$; ANOVA), even though individual wild-type larvae were not significantly different from each other ($p < 0.2$; ANOVA). Data from the identified neuromuscular synapse fully corroborated the CNS data. Taken together, these data indicate that synaptotagmin function is required to achieve wild-type levels of morphological docking.

The decreased number of morphologically docked vesicles cannot be accounted for by overall vesicle depletion. First, the overall number of synaptic vesicles near synapses in syt^{null} (the mutant with the most severe depletion) is reduced to 48% of control, but morphologically docked vesicles are reduced further to 24% of control. Second, the number of vesicles near but not touching the presynaptic membrane (the 18–50 nm bin; see Fig. 5*B*) is reduced to only 73% of control; thus, the neighboring supply of vesicles shows the least depletion. Third, neuromuscular junctions in the *$,syt^{AD3}$/*$,syt^{null}$ mutants exhibit a decrease in the docked pool of vesicles even though there was a slight increase in the total number of vesicles nearby.

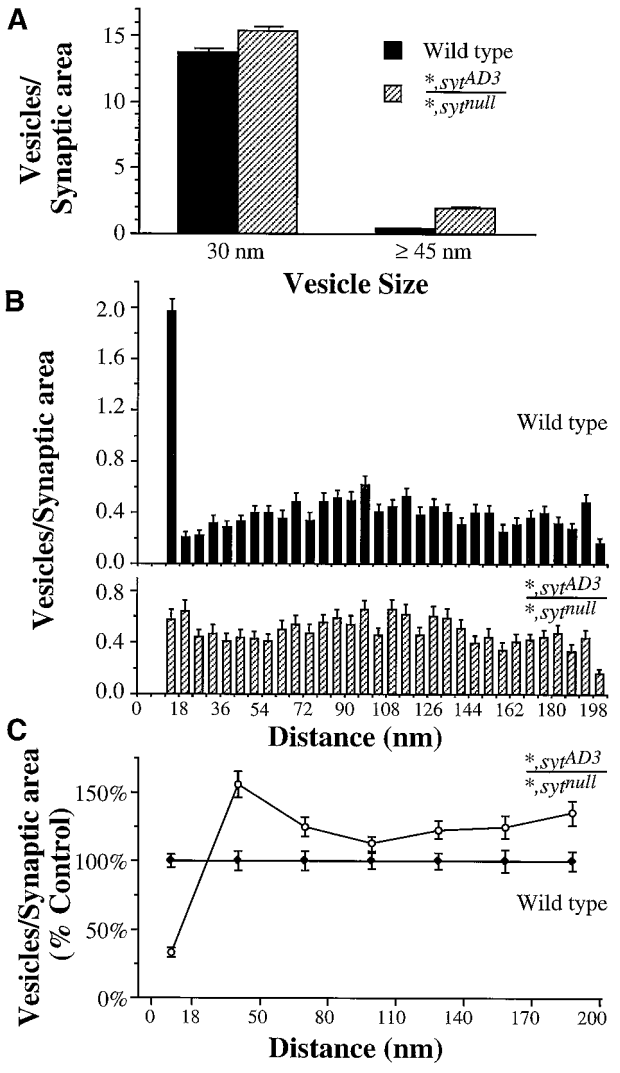

Figure 9. The number and distribution of synaptic vesicles in the vicinity of dense bodies. The distance of vesicles from the presynaptic membrane was determined as shown in Figure 8*B*. *A*, The overall number of synaptic vesicles and large vesicles in the vicinity of dense bodies was increased slightly in $*,syt^{AD3}/*,syt^{null}$ mutants as compared with wild-type (means ± SEM; $n = 91$ wild-type synapses and 106 mutant synapses; $p < 0.01$; Student's *t* test). *B*, A histogram showing the number of synaptic vesicles versus the distance from the presynaptic membrane for wild-type and $*,syt^{AD3}/*,syt^{null}$ mutants (means ± SEM). For a comparison of the vesicle population at each distance, the data were plotted as a percentage of the wild-type control (*C*). As in Figure 5*B*, the 12–18 nm bin, which is likely to represent docked vesicles, was kept separate, whereas the rest of the bins were enlarged to one vesicle diameter, 30 nm, to reduce random scatter. The number of docked vesicles is reduced markedly in $*,syt^{AD3}/*,syt^{null}$ mutants ($p \ll 0.001$; Student's *t* test), even though the overall number of synaptic vesicles near synapses is elevated slightly in this genotype.

A similar analysis reveals that the decrease in docking is also independent of the rate of spontaneous release. syt^{null} and syt^{AD3}/syt^{null} both exhibit an increased rate of spontaneous release (Broadie et al., 1994; DiAntonio and Schwarz, 1994), whereas $*,syt^{AD3}/*,syt^{null}$ does not (see Fig. 7*B*), yet the number of morphologically docked vesicles is decreased in all three. Thus, the effect of synaptotagmin on morphological docking is not secondary to vesicle depletion or an increased rate of spontaneous release but appears to be a primary function of synaptotagmin.

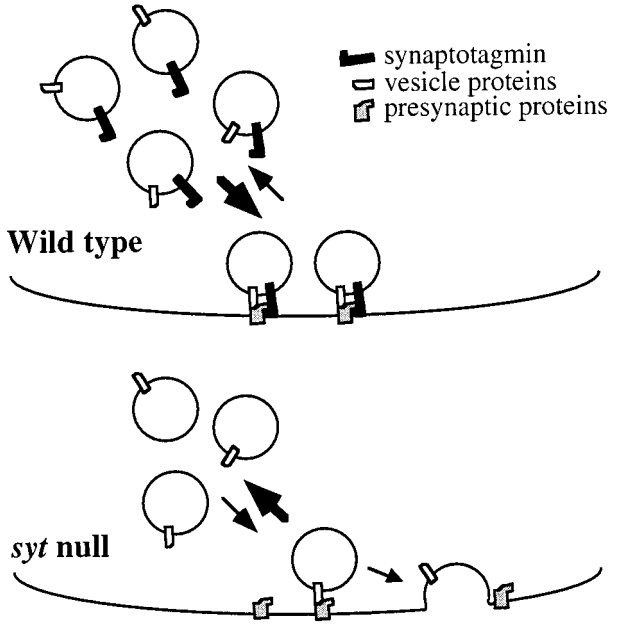

Figure 10. Synaptotagmin may stabilize the docked state via its interactions with other synaptic vesicle and presynaptic membrane proteins. In *synaptotagmin* mutants there is a decrease in the number of docked vesicles. The model proposes that, in the absence of synaptotagmin, the stability of the docked state is reduced. This may be attributable to one or more of the following: (1) a decrease in the ability of the release site to capture nearby vesicles, (2) a decrease in the ability to retain vesicles, and (3) an increase in the rate of spontaneous release of those vesicles that do bind.

Synaptotagmin is important for efficient coupling of presynaptic activity to transmitter release. In *syt* mutants the evoked release is reduced to ~10% of control, and the rate of spontaneous fusions is increased three- to fivefold (Broadie et al., 1994; DiAntonio and Schwarz, 1994). Evidence that synaptotagmin is a Ca^{2+}-binding protein and therefore may serve as a Ca^{2+} sensor has overshadowed the potential role of synaptotagmin in vesicle docking (Bennett et al., 1992; Schiavo et al., 1997). However, synaptotagmin has been shown to interact with the presynaptic membrane proteins syntaxin (Bennett et al., 1992; Chapman et al., 1996; Kee and Scheller, 1996) and SNAP-25 (Schiavo et al., 1997), suggesting that synaptotagmin may help to anchor vesicles at release sites. Indeed, the persistence of morphologically docked vesicles in the presence of tetanus toxin, which cleaves some isoforms of VAMP/synaptobrevin (Hunt et al., 1994; Broadie et al., 1995), suggests that another vesicle protein or proteins may function during docking; synaptotagmin is an excellent candidate (Schiavo et al., 1997). Our ultrastructural results support the hypothesis that synaptotagmin plays a direct role in vesicle docking.

The overall depletion in synaptic vesicles and the increased number of large vesicles seen in some *syt* mutant terminals are consistent with the hypothesis that vesicle recycling or biosynthesis also may be compromised [as suggested for *syt* mutants of *C. elegans* (Jorgensen et al., 1995)]. This depletion is particularly apparent in the null mutant, in which the absence of a major vesicle protein may decrease the efficacy of synaptic vesicle formation. The increased rate of spontaneous release seen in these mutants also may contribute to the overall vesicle depletion. The precise nature of the large irregular vesicles is not yet known; they may represent recently retrieved membrane, excess endo-

somes, or incorrectly assembled synaptic vesicles. At CNS synapses they may account for much of the membrane that is missing from the reduced small vesicle pool. However, further studies of *syt* mutants that use vesicle tracers, such as HRP or FM 1–43, will be necessary to determine whether any of these large vesicles are part of the synaptic vesicle cycle.

We propose a model (Fig. 10) in which one function of synaptotagmin is to stabilize vesicles in the docked state. This could be accomplished by one or more of the following mechanisms: (1) by increasing the recruitment of vesicles from the cytoplasm to docking sites (positive recruitment), (2) by preventing the vesicle from dissociating from docking sites (retention), and (3) by preventing these vesicles from fusing before stimulated release (negative regulator of spontaneous release). Because the reduction in morphologically docked vesicles was independent of the rate of spontaneous fusions, synaptotagmin appears to preserve the docked state directly. In addition, the increase in spontaneous release suggests that those vesicles that dock in *syt* mutants have an increased probability of spontaneously "fusing." A deficit in docking stability, as proposed in our model, can account for both of the electrophysiological defects seen in *syt* mutants: decreased EJP size and increased rate of spontaneous release.

The dramatic decrease that we observed in vesicles immediately adjacent to the presynaptic membrane contrasts with the increase seen when synaptotagmin-based peptides were injected into squid terminals (Bommert et al., 1993). This discrepancy may be attributable to several causes. The intracellular actions of the peptides are uncertain at present; they may mimic synaptotagmin and promote docking, whereas the mutations, which disrupt synaptotagmin, reduce docking. Alternatively, the discrepancy may arise from the difference between blocking a portion of the protein and deleting it entirely, particularly if distinct domains of the protein mediate distinct functions in the vesicle cycle. For example, the acutely applied peptide acts on vesicles that have assembled correctly and contain synaptotagmin, whereas the mutations reveal that normal vesicle number and distribution require synaptotagmin.

The recruitment of vesicles to release sites by synaptotagmin may be Ca^{2+}-dependent, consistent with the observed Ca^{2+}-dependent translocation of a synaptotagmin C2 domain to the membrane (Chapman and Jahn, 1994) and the role of C2 domains in translocation of protein kinase C and phospholipase A2 to membranes. Additional effects of Ca^{2+} binding to synaptotagmin may act downstream of docking and promote membrane fusion. Analyzing more mutations may help to determine which biochemical interactions with synaptic proteins accomplish the stabilization of the docked state.

REFERENCES

Bate M, Martinez Arias A, Editors (1993) The development of *Drosophila melanogaster*. Plainview, NY: Cold Spring Harbor Laboratory.

Bennett MK, Calakos N, Scheller RH (1992) Syntaxin: a synaptic protein implicated in docking of synaptic vesicles at presynaptic active zones. Science 257:255–259.

Bommert K, Charlton MP, DeBello WM, Chin GJ, Betz H, Augustine GJ (1993) Inhibition of neurotransmitter release by C2-domain peptides implicates synaptotagmin in exocytosis. Nature 363:163–165.

Broadie K, Bellen HJ, DiAntonio A, Littleton JT, Schwarz TL (1994) Absence of synaptotagmin disrupts excitation–secretion coupling during synaptic transmission. Proc Natl Acad Sci USA 91:10727–10731.

Broadie K, Prokop A, Bellen HJ, O'Kane CJ, Schulze KL, Sweeney ST (1995) Syntaxin and synaptobrevin function downstream of vesicle docking in *Drosophila*. Neuron 15:663–673.

Brose N, Petrenko AG, Sudhof TC, Jahn R (1992) Synaptotagmin: a calcium sensor on the synaptic vesicle surface. Science 256:1021–1025.

Budnik V, Zhong Y, Wu C-F (1990) Morphological plasticity of motor axons in *Drosophila* mutants with altered excitability. J Neurosci 10:3754–3768.

Chapman ER, Jahn R (1994) Calcium-dependent interaction of the cytoplasmic region of synaptotagmin with membranes. Autonomous function of a single C2-homologous domain. J Biol Chem 269:5735–5741.

Chapman ER, Hanson PI, An S, Jahn R (1995) Ca^{2+} regulates the interaction between synaptotagmin and syntaxin 1. J Biol Chem 270:23667–23671.

Chapman ER, An S, Edwardson JM, Jahn R (1996) A novel function for the second C2 domain of synaptotagmin. Ca^{2+}-triggered dimerization. J Biol Chem 271:5844–5849.

Clark JD, Lin LL, Kriz RW, Ramesha CS, Sultzman LA, Lin AY, Milona N, Knopf JL (1991) A novel arachidonic acid-selective cytosolic PLA2 contains a Ca^{2+}-dependent translocation domain with homology to PKC and GAP. Cell 65:1043–1051.

Couteaux R, Pecot-Dechavassine M (1973) Donnees ultrastructurales et cytochimiques sur le mecanisme de liberation de l'acetylcholine dans la transmission synaptique. Arch Ital Biol 3:231–262.

DiAntonio A, Schwarz TL (1994) The effect on synaptic physiology of synaptotagmin mutations in *Drosophila*. Neuron 12:909–920.

DiAntonio A, Burgess RW, Chin AC, Deitcher DL, Scheller RH, Schwarz TL (1993a) Identification and characterization of *Drosophila* genes for synaptic vesicle proteins. J Neurosci 13:4924–4935.

DiAntonio A, Parfitt KD, Schwarz TL (1993b) Synaptic transmission persists in synaptotagmin mutants of *Drosophila*. Cell 73:1281–1290.

Elferink LA, Peterson MR, Scheller RH (1993) A role for synaptotagmin (p65) in regulated exocytosis. Cell 72:153–159.

Geppert M, Goda Y, Hammer RE, Li C, Rosahl TW, Stevens CF, Sudhof TC (1994) Synaptotagmin I: a major Ca^{2+} sensor for transmitter release at a central synapse. Cell 79:717–727.

Hall D, Hedgecock E (1991) Kinesin-related gene *unc-104* is required for axonal transport of synaptic vesicles in *C. elegans*. Cell 65:837–847.

Hunt J, Bommert K, Charlton M, Kistner A, Habermann E, Augustine G, Betz H (1994) A post-docking role for synaptobrevin in synaptic vesicle fusion. Neuron 12:1269–1279.

Jan LY, Jan YN (1976) Properties of the larval neuromuscular junction in *Drosophila melanogaster*. J Physiol (Lond) 262:189–214.

Jorgensen EM, Hartwieg E, Schuske K, Nonet ML, Jin Y, Horvitz HR (1995) Defective recycling of synaptic vesicles in synaptotagmin mutants of *Caenorhabditis elegans*. Nature 378:196–199.

Kee Y, Scheller RH (1996) Localization of synaptotagmin-binding domains on syntaxin. J Neurosci 16:1975–1981.

Koenig J, Yamaoka K, Ikeda K (1993) Calcium-induced translocation of synaptic vesicles to the active site. J Neurosci 13:2313–2322.

Littleton JT, Bellen HJ, Perin MS (1993a) Expression of synaptotagmin in *Drosophila* reveals transport and localization of synaptic vesicles to the synapse. Development 118:1077–1088.

Littleton JT, Stern M, Schulze K, Perin M, Bellen HJ (1993b) Mutational analysis of *Drosophila* synaptotagmin demonstrates its essential role in Ca^{2+}-activated neurotransmitter release [see comments]. Cell 74:1125–1134.

Mastrogiacomo A, Parsons SM, Zampighi GA, Jenden DJ, Umbach JA, Gundersen CB (1994) Cysteine string protein: a potential link between synaptic vesicles and presynaptic Ca^{2+} channels. Science 263:981–982.

Mochly RD, Miller KG, Scheller RH, Khaner H, Lopez J, Smith BL (1992) p65 fragments, homologous to the C2 region of protein kinase C, bind to the intracellular receptors for protein kinase C. Biochemistry 31:8120–8124.

Nonet ML, Grundahl K, Meyer BJ, Rand JB (1993) Synaptic function is impaired but not eliminated in *C. elegans* mutants lacking synaptotagmin. Cell 73:1291–1305.

O'Connor V, Heuss C, Bello WM, Dresbach T, Charlton MP, Hunt JH, Pellegrini LL, Hodel A, Burger MM, Betz H (1997) Disruption of syntaxin-mediated protein interactions blocks neurotransmitter secretion. Proc Natl Acad Sci USA 94:12186–12191.

Perin MS, Fried VA, Mignery GA, Jahn R, Sudhof TC (1990) Phospholipid binding by a synaptic vesicle protein homologous to the regulatory region of protein kinase C. Nature 345:260–263.

Peters A, Palay SL, Webster H (1991) Fine structure of the nervous system. New York: Oxford UP.

Petrenko AG, Perin MS, Davletov BA, Ushkaryov YA, Geppert M,

Sudhof TC (1991) Binding of synaptotagmin to the α-latrotoxin receptor implicates both in synaptic vesicle exocytosis. Nature 353:65–68.

Sato T (1968) A modified method for lead staining of thin sections. J Electron Microsc Tech 17:158–159.

Schiavo G, Stenbeck G, Rothman J, Sollner T (1997) Binding of the synaptic vesicle v-SNARE, synaptotagmin, to the plasma membrane t-SNARE, SNAP-25, can explain docked vesicles at neurotoxin-treated synapses [see comments]. Proc Natl Acad Sci USA 94:997–1001.

Shao X, Davletov BA, Sutton RB, Sudhof TC, Rizo J (1996) Bipartite Ca^{2+}-binding motif in C2 domains of synaptotagmin and protein kinase C. Science 273:248–251.

Shao X, Li C, Fernandez I, Zhang X, Sudhof T, Rizo J (1997) Synaptotagmin–syntaxin interaction: the C2 domain as a Ca^{2+}-dependent electrostatic switch. Neuron 18:133–142.

Sollner T, Bennett MK, Whiteheart SW, Scheller RH, Rothman JE (1993) A protein assembly–disassembly pathway *in vitro* that may correspond to sequential steps of synaptic vesicle docking, activation, and fusion. Cell 75:409–418.

Stewart BA, Atwood HL, Renger JJ, Wang J, Wu C-F (1994) Improved stability of *Drosophila* larval neuromuscular preparations in haemolymph-like physiological solutions. J Comp Physiol [A] 175:179–191.

Sutton RB, Davletov BA, Berghuis AM, Sudhof TC, Sprang SR (1995) Structure of the first C2 domain of synaptotagmin I: a novel Ca^{2+}/phospholipid-binding fold. Cell 80:929–938.

Weibel ER (1979) Stereological methods. Practical methods for biological morphometry. New York: Academic.

Wendland B, Miller KG, Schilling J, Scheller RH (1991) Differential expression of the *p65* gene family. Neuron 6:993–1007.

Zhang JZ, Davletov BA, Sudhof TC, Anderson RG (1994) Synaptotagmin I is a high-affinity receptor for clathrin AP-2: implications for membrane recycling. Cell 78:751–760.

Zinsmaier KE, Eberle KK, Buchner E, Walter N, Benzer S (1994) Paralysis and early death in cysteine string protein mutants of *Drosophila*. Science 263:977–980.